COMMUNICATIONS IN NUMERICAL METHODS IN ENGINEERING
Commun. Numer. Meth. Engng 2008; **24**:49–63
Published online 20 November 2006 in Wiley InterScience (www.interscience.wiley.com). DOI: 10.1002/cnm.955

A Taylor–Galerkin approach for modelling a spherically symmetric advective–dispersive transport problem

Wenjun Dong and A. P. S. Selvadurai*, †

Department of Civil Engineering and Applied Mechanics, McGill University, 817 Sherbrooke Street West, Montreal, Canada QC H3A 2K6

SUMMARY

This paper presents a numerical approach for examining a spherically symmetric advective–dispersive contaminant transport problem. The Taylor–Galerkin method that is based on an Euler time-integration scheme is used to solve the governing transport equation. A Fourier analysis shows that the Taylor–Galerkin method with a forward Euler time integration can generate an oscillation-free and non-diffusive solution for the pure advection equation when the Courant number satisfies the constraint $Cr = 1$. Such numerical advantages, however, do not extend to the advection–dispersion equation. Based on these observations, an operator-splitting Euler-integration-based Taylor–Galerkin scheme is developed to model the advection-dominated transport process for a problem that exhibits spherical symmetry. The spherically symmetric transport problem is solved using this approach and a conversion to a one-dimensional linear space with an associated co-ordinate transformation. Copyright © 2006 John Wiley & Sons, Ltd.

Received 7 March 2006; Revised 25 September 2006; Accepted 3 October 2006

KEY WORDS: advection–dispersive transport; Euler–Taylor–Galerkin method; Fourier analysis; Courant number; operator-splitting approach

1. INTRODUCTION

The study of the time- and space-dependent migration of contaminants in porous media is an important topic in geoenvironmental engineering, particularly for contaminant management and to assist in the decision-making process in endeavours such as groundwater remediation and soil clean-up [1, 2]. Although contaminant transport in porous media involves complex nonlinear processes, which are usually influenced by the complex mechanical behaviour of the porous medium, thermal effects and geochemical phenomena [3, 4], the simplest approach to the study of contaminant transport still relies on the conventional advection–dispersion (or diffusion) equation. The solution of practical problems dealing with such coupling effects invariably requires accurate

*Correspondence to: A. P. S. Selvadurai, William Scott Professor and James McGill Professor, Department of Civil Engineering and Applied Mechanics, McGill University, Montreal, QC H3A 2K6, Canada.
†E-mail: patrick.selvadurai@mcgill.ca

and reliable computational approaches. In this context, finite element methods have been widely used to solve the advective–dispersive transport problem. The conventional Galerkin discretization is equivalent to the central difference approximation for the differential operator, and therefore, it is unconditionally unstable for the first-order hyperbolic problem in the sense that it introduces spurious oscillations or wiggles into the solution near high gradients. A solution that contains the sharp gradient or discontinuity is equivalent to the step wave. In the frequency domain, such step wave is composed of wave components of different frequencies and should include high-frequency wave components. If a numerical scheme is used to simulate the propagation of such a step wave, the amplitudes and phase velocities of the wave components (especially high-frequency wave components) of the step wave can be altered by the numerical scheme. Such alterations can make wave components possess different propagation velocities and propagation profiles, resulting in oscillations during the propagation of the step wave. From this point of view, Fourier analysis can provide an insight into numerical properties of the scheme in the frequency domain by illustrating the variation of the algorithmic amplitude and phase velocity of the scheme [5–10].

In the conventional finite element space employed in the Galerkin approach, a polynomial is used to construct the shape function and to interpolate the unknown variable over the computational domain. Such a polynomial space can interpret low-frequency wave components involved in the solution, which can be referred to as the *resolvable coarse scales* of the solution. It can, however, be inadequate for capturing the high-frequency wave components involved in a solution containing a discontinuity, which can be considered as the *unresolvable fine-scales* (or *subgrid-scales*) of solution [11]. Therefore, the polynomial finite element space should be augmented by a higher-order function space. The space of the *bubble function* is one choice that can take into consideration such fine-scale effects in a solution [12]. The bubble functions are typically higher-order polynomial functions which vanish on the elemental boundaries [13], and in this sense, they are referred to as the *residual-free bubbles* [14]. Usually, the bubble functions are constructed by solving a certain element-level homogeneous Dirichlet boundary value problem [15], and therefore, this approach requires a greater computational effort.

Another approach for taking into account such fine-scale effects involved in a solution is to consider its effect on the coarse scale of the solution in the normal polynomial finite element space by means of an elemental Green's function [11], which results in the addition of a stabilization term to the standard weighted residual integral form of the Galerkin method for the advection–dispersion equation [10, 16]. Since the coarse-scale of the solution in the normal finite element space is of more interest for most engineering applications, this approach has been considered for over three decades, and many stabilized semi-discrete finite element methods, such as the streamline upwind Petrov–Galerkin method [17], the least-squares method [18] and the Taylor–Galerkin method [19] follow the general stabilized weighted residual integral form led by the multi-scale concept and the elemental Green's function approach mentioned above [9, 10]. The differences in these stabilized finite element methods are due to the different definitions of the stabilized parameter involved [16]. The stabilized parameter can be determined by a Fourier analysis such that the stabilized finite element method has an optimal performance for the transport equation.

In this paper, a Fourier analysis is used to investigate the numerical performance of a Taylor–Galerkin method with an Euler time-integration scheme [19, 20] that is used to solve the advection–dispersion equation. Based on this investigation, an operator-splitting approach is proposed for modelling a spherically symmetric advection-dominated contaminant transport problem. The structure of the paper is described as follows: Section 2 gives the formulation of the contaminant transport problem referred to a spherically symmetric co-ordinate system. Section 3

DOI: 10.1002/cnm

describes the Euler–Taylor–Galerkin (ETG) method for examining the classical advection–dispersion equation. A Fourier analysis presented in Section 4 shows that the ETG scheme can provide an accurate solution of the advection equation with a Courant number criterion $Cr = 1$, but such a numerical advantage does not extend to the solution of the advection–dispersion equation. The numerical computations presented in Section 5 confirm the results of the Fourier analysis. Section 6 presents an operator-splitting ETG scheme for modelling the advection-dominated transport from a spherical cavity in a fluid saturated isotropic porous region. In this modelling, a co-ordinate transformation is used to reduce the spherically symmetric problem to an alternative spatially one-dimensional formulation, which is solved using the ETG scheme.

2. SPHERICALLY SYMMETRIC CONTAMINANT TRANSPORT

Attention is focused on the advective–dispersive contaminant transport problem referred to a spherical cavity of radius $a (a > 0)$ located in an isotropic fluid-saturated porous region (Figure 1). For incompressible fluid flow, the partial differential equation governing the spherically symmetric contaminant transport has the form

$$\frac{\partial C}{\partial t} + v_{\mathrm{R}} \frac{\partial C}{\partial R} - D \nabla_{\mathrm{R}}^2 C = 0 \tag{1}$$

where $C(R, t)$ is the scalar concentration of the contaminant; R is the spherical polar co-ordinate; t is time; v_{R} is the averaged advective flow velocity in the pore space along the radial direction; D is hydrodynamic dispersion coefficient; ∇_{R}^2 is Laplace's operator defined by $\nabla_{\mathrm{R}}^2 = \partial^2/\partial R^2 + 2/R\partial/\partial R$.

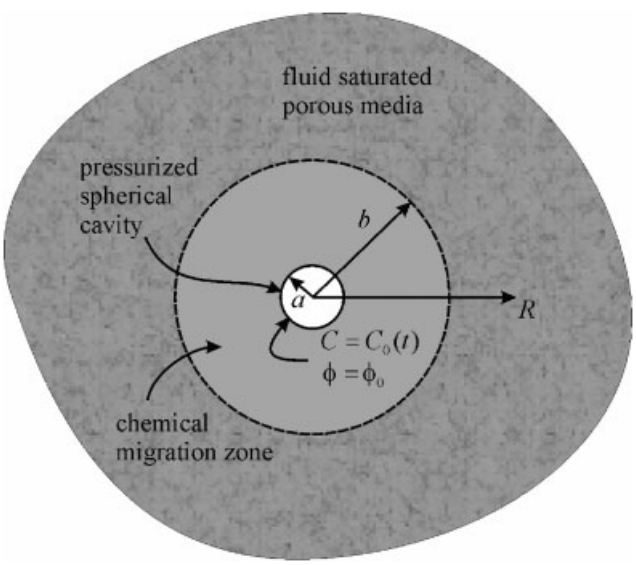

Figure 1. A schematic drawing of the contaminant transport from a spherical cavity for deep geological disposal of hazardous chemicals.

DOI: 10.1002/cnm

The last term in the left-hand side of (1) corresponds to the dispersion along the spherically radial direction. In addition to the governing equation, the contaminant movement in an extended porous medium $R \in (a, \infty)$ is subject to the following boundary and the regularity conditions

$$C(a, t) = C_0 \mathsf{H}(t); \quad C(\infty, t) \to 0 \tag{2}$$

as well as the initial condition

$$C(R, 0) = 0; \quad R \in [a, \infty) \tag{3}$$

In (2), C_0 is a constant chemical concentration and $\mathsf{H}(t)$ is a Heaviside function.

The radial flow velocity v_{R} can be determined from the flow potential ϕ_{p} and Darcy's law. For spherically symmetric incompressible flow in a rigid porous medium, the flow potential ϕ_{p} satisfies Laplace's equation

$$\frac{\mathrm{d}^2\phi_{\mathrm{p}}}{\mathrm{d}R^2} + \frac{2}{R}\frac{\mathrm{d}\phi_{\mathrm{p}}}{\mathrm{d}R} = 0 \tag{4}$$

If the medium containing the spherical cavity is unbounded, the appropriate boundary and regularity conditions for ϕ_{p} are

$$\phi_{\mathrm{p}}(a) = \phi_0; \quad \phi_{\mathrm{p}}(\infty) \to 0 \tag{5}$$

Therefore, the steady radial flow velocity can be determined as

$$v_{\mathrm{R}} = -k\frac{\mathrm{d}\phi_{\mathrm{p}}}{\mathrm{d}R} = k\frac{a\phi_0}{R^2} \tag{6}$$

where k is the Dupuit–Forchheimer hydraulic conductivity that is related to the conventional area-averaged hydraulic conductivity $\tilde{k}$ by the relation $k = \tilde{k}/n^*$ and n^* is the porosity of the porous medium. We should note that the advective velocity v_{R} is finite and bounded for any three-dimensional domain $a \leqslant R < \infty$, where a is a finite length parameter.

3. NUMERICAL FORMULATION

3.1. Stabilized weighted residual form

The basic approach for developing a stabilized finite element method is to add a perturbation to the standard weighting function to account for the fine scales involved in the solution. The addition of such a perturbation term is equivalent to adding a stabilization term to the weighted residual integral form of the advection–dispersion equation (1) [16], i.e.

$$\int_V wL(C^h)\,\mathrm{d}V + \sum_{e=1}^{n_{el}} \int_{V^e} \ell(w)\tau L(C^h)\,\mathrm{d}V = 0 \tag{7}$$

where $L = \partial/\partial t + v_{\mathrm{R}}\partial/\partial R - D\nabla_{\mathrm{R}}^2$; w and C^h are, respectively, the weighting function and trial solution on the elemental space $\bigcup_{e=1}^{n_{\mathrm{el}}} V^e$, n_{el} is total number of elements, τ is a matrix of stabilized parameters (called the intrinsic time) with dimension of time [21] and ℓ is a typical differential operator applied to the test function. Different definitions of the intrinsic time and

DOI: 10.1002/cnm

different forms of the differential operator ℓ will lead to different stabilized numerical schemes for the advection–dispersion equation (1), such as the streamline upwind Petrov–Galerkin method [17] and the least-squares method [18].

It should be noted that the integrals involved in the stabilized residual integral form (7) are defined in relation to the spherical co-ordinate system (R, ϕ, θ). Due to spherical symmetry of (1), these integrals are performed over the cubic space R^3 as follows:

$$\int_V F(R)\,\mathrm{d}V = \int_0^{2\pi}\int_0^{\pi}\int_a^{\infty} F(R)R^2\sin\phi\,\mathrm{d}R\,\mathrm{d}\phi\,\mathrm{d}\theta = 4\pi\int_a^{\infty} F(R)\,\mathrm{d}\left(\frac{R^3}{3}\right) \tag{8}$$

where $F(R)$ represents the integral functions in (7). These integrals over the cubic space R^3 can be converted to linear integrals using the co-ordinate transformation

$$x = R^3/3 \tag{9}$$

Using (9), the spherically symmetric advection–dispersion equation (1) can be transformed to its counterpart expressed by a one-dimensional rectangular Cartesian co-ordinate x as follows:

$$\frac{\partial C}{\partial t} + u\frac{\partial C}{\partial x} - D(3\sqrt[3]{3x})\left(2\frac{\partial C}{\partial x} + x\frac{\partial^2 C}{\partial x^2}\right) = 0 \tag{10}$$

where $u = R^2 v_{\mathrm{R}} = ka\phi_0$ is the transformed advective flow velocity that is *constant* only in the case of spherical symmetry. The last term in the left-hand side of (10) represents the spherically radial dispersion. It is evident from (10) that the spherically symmetric advective–dispersive transport problem governed by (1) can be computed in the one-dimensional space referred to the Cartesian co-ordinate x.

3.2. The Euler–Taylor–Galerkin method

A specific expression for the stabilized residual integral form can be derived from a Taylor–Galerkin method with Euler time integration scheme [19] for the classical advection–dispersion equation

$$\frac{\partial C}{\partial t} + u\frac{\partial C}{\partial x} - D\frac{\partial^2 C}{\partial x^2} = 0 \tag{11}$$

The basic concept underlying the Euler scheme based Taylor–Galerkin method originates from the Lax–Wendroff finite difference scheme [22] in which a forward time Taylor series expansion of the unknown variable is used in Euler discretization of the temporal derivative of the advection–dispersion equation to obtain a greater accuracy in time, i.e.

$$C^{n+1} = C^n + \frac{\partial C}{\partial t}\Delta t + \frac{1}{2}\frac{\partial^2 C}{\partial t^2}\Delta t^2 + \frac{1}{6}\frac{\partial^3 C}{\partial t^3}\Delta t^3 + O(\Delta t^4) \tag{12}$$

DOI: 10.1002/cnm

Assuming that the differentiation with respect to x and t commute, successive differentiations of (11) give

$$\frac{\partial^2 C}{\partial t^2} = u^2 \frac{\partial^2 C}{\partial x^2} - 2uD \frac{\partial^3 C}{\partial x^3} + D^2 \frac{\partial^4 C}{\partial x^4} \tag{13a}$$

$$\frac{\partial^3 C}{\partial t^3} = u^2 \frac{\partial^2}{\partial x^2} \frac{\partial C}{\partial t} - \left(2uD \frac{\partial^3}{\partial x^3} - D^2 \frac{\partial^4}{\partial x^4} \right) \frac{\partial C}{\partial t} \tag{13b}$$

Combining (12) with (13) and omitting terms of spatial derivatives higher than the third order, we obtain a stabilized equation with Euler (forward) time marching scheme as follows [20]:

$$\left(1 - \frac{\Delta t^2}{6} u^2 \frac{\partial^2}{\partial x^2} \right) \frac{C^{n+1} - C^n}{\Delta t} + u \frac{\partial C^n}{\partial x} = \frac{\Delta t}{2} u^2 \frac{\partial^2 C^n}{\partial x^2} + D \frac{\partial^2 C^n}{\partial x^2} \tag{14}$$

Equation (14) shows that the additional terms of the Taylor series introduces not only an *artificial diffusion* term (the last term on the right-hand side of the equation) but also an *artificial advection* term (the second term in the bracket with the Euler time-integration scheme on the left-hand side of the equation) to the original advection–dispersion equation. Applying the standard Galerkin scheme with linear elements to (14) gives a weak form of the ETG method for the advection–dispersion equation (11) as follows:

$$\int_V \left[w + \frac{\Delta t^2}{6} u^2 \frac{\mathrm{d}w}{\mathrm{d}x} \frac{\partial}{\partial x} \right] \frac{C^{n+1} - C^n}{\Delta t} \, \mathrm{d}x + \int_V \left[wu + \left(\frac{\Delta t}{2} u^2 + D \right) \frac{\mathrm{d}w}{\mathrm{d}x} \right] \frac{\partial C^n}{\partial x} \, \mathrm{d}x = 0 \tag{15}$$

It should be noted from the integral form (15) that the stabilized terms corresponding to the artificial advection and artificial diffusion terms in (14) can be introduced by adding a perturbation term to the standard Galerkin weighting function, and the perturbation for the temporal term is different from that for the spatial term of the governing equation. The effect of the stabilized terms on the numerical performance of the resulting ETG method for the advection–dispersion equation can be investigated by a Fourier analysis.

4. A FOURIER ANALYSIS OF THE EULER–TAYLOR–GALERKIN METHOD

The finite difference stencil of (15) with a piecewise linear element of length h can be written as

$$C_j^{n+1} = C_j^n + \Delta t \, \mathbf{A} C_j^n \tag{16}$$

where $\mathbf{A} = \mathbf{A}_1^{-1} \cdot \mathbf{A}_2$ and $\mathbf{A}_i$ $(i = 1, 2)$ are the spatial discrete operators defined by

$$\mathbf{A}_1 = \frac{1}{6}(C_{j-1} + 4C_j + C_{j+1}) - \frac{\Delta t^2 u^2}{6h^2}(C_{j-1} - 2C_j + C_{j+1}) \tag{17a}$$

$$\mathbf{A}_2 = -\frac{u}{2h}(C_{j+1} - C_{j-1}) + \frac{1}{h^2}\left(\frac{\Delta t u^2}{2} + D \right)(C_{j-1} - 2C_j + C_{j+1}) \tag{17b}$$

DOI: 10.1002/cnm

The harmonic solution of (16) can be written as

$$C_j^n = C(x_j, t_n) = \exp[\mathrm{i}\omega x_j - v^h t_n] = \exp[-\xi^h t_n] \exp\left[\mathrm{i}\omega\left(x_j - \frac{\Omega^h}{\omega} t_n\right)\right] \tag{18}$$

where $h = x_{j+1} - x_j$ is the spatial increment, $\Delta t = t^{n+1} - t^n$ is the temporal increment, ω is the spatial wave number, $v^h = \xi^h + \mathrm{i}\Omega^h$ determines the temporal evolution of the solution, ξ^h and Ω^h are, respectively, the *numerical damping coefficient* and the *wave frequency* corresponding to the spatial increment h. Substituting (18) into (16) gives

$$[\zeta^h \mathrm{e}^{-\mathrm{i}\Omega^h \Delta t}] C_j^n = z(\omega) C_j^n \tag{19}$$

where $z(\omega)$ is the *spectral function* of the numerical operator presented in (16), defined as follows:

$$z(\omega) = \frac{[2 + \cos(\omega h)] - 2Cr[Cr + 3Pe^{-1}][1 - \cos(\omega h)] - \mathrm{i}3Cr \sin(\omega h)}{[2 + \cos(\omega h)] + Cr^2[1 - \cos(\omega h)]} \tag{20}$$

In (20), Cr $(= u\Delta t / h)$ is the Courant number and Pe $(= uh/D)$ is the Péclet number. From (19) and (20), the *amplification factor* ζ^h and *relative phase velocity* u^*/u of the ETG method for the advection–dispersion equation can be determined as follows:

$$\zeta^h = |z(\omega)| = \frac{\sqrt{[(2 + \cos(\omega h)) - 2Cr(Cr + 3Pe^{-1})(1 - \cos(\omega h))]^2 + 9Cr^2 \sin^2(\omega h)}}{[2 + \cos(\omega h)] + Cr^2[1 - \cos(\omega h)]} \tag{21}$$

$$\frac{u^*}{u} = \frac{\Omega^h}{\omega} = -\frac{\arg(z(\omega))}{\omega \Delta t} = \frac{1}{Cr\,\omega h} \tan^{-1}\left(\frac{3Cr \sin(\omega h)}{[2 + \cos(\omega h)] - 2Cr[Cr + 3Pe^{-1}][1 - \cos(\omega h)]}\right) \tag{22}$$

It is evident from the definitions shown in (21) and (22), that the Courant number and the Péclet number have an influence on the amplification factor and the relative phase velocity of the ETG method for the advection–dispersion equation.

When $D = 0$ (or $Pe^{-1} = 0$), Equations (21) and (22) represent the variations of the amplification factor ζ^h and the relative phase velocity u^*/u of the ETG method for the advection equation with the dimensionless wave number ωh and the Courant number Cr, which are shown in Figure 2. It should be noted from Figure 2 that when $Pe^{-1} = 0$ and $Cr = 1$, both ζ^h and u^*/u of the ETG method for the advection equation are equal to unity for all ωh. In fact, keeping $Pe^{-1} = 0$ and $Cr = 1$ in (21) and (22) gives

$$\zeta^h|_{Pe^{-1}=0, Cr=1} = 1 \tag{23}$$

$$\left.\frac{u^*}{u}\right|_{Pe^{-1}=0, Cr=1} = 1 \tag{24}$$

It follows from (23) and (24) that when $Pe^{-1} = 0$ and $Cr = 1$, no errors will be introduced in ζ^h and u^*/u of the ETG method for the advection equation for all ωh, and all wave components

DOI: 10.1002/cnm

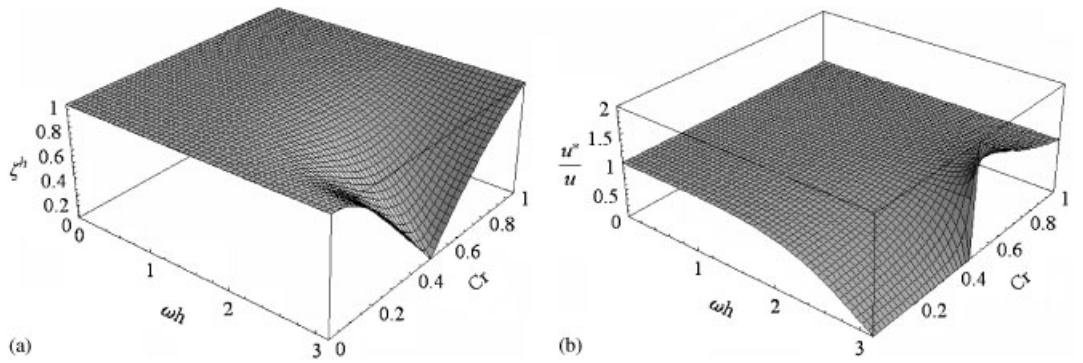

Figure 2. The variations of the amplification factor and relative phase velocity of the ETG method for the advection equation with ωh and Cr: (a) amplification factor; and (b) relative phase velocity.

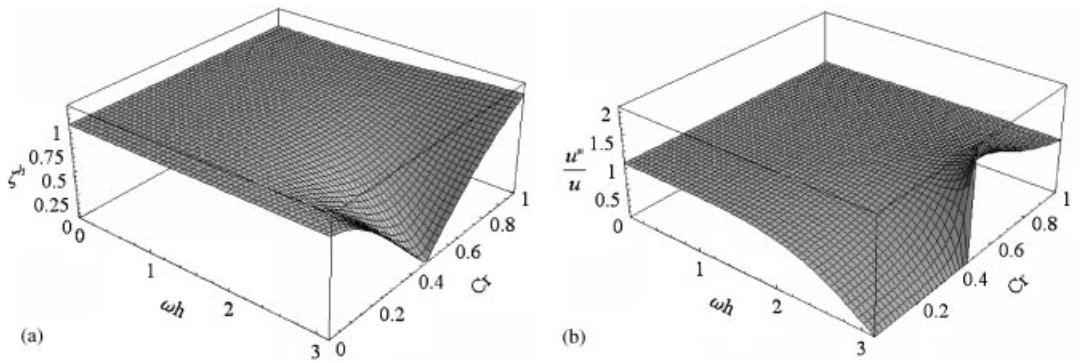

Figure 3. The variations of the amplification factor and the relative phase velocity of the ETG method for the advection–dispersion equation with ωh and Cr corresponding to $Pe = 50$: (a) amplification factor; and (b) relative phase velocity.

included in the solution will therefore travel at the same speed and without the distortion. This implies that the ETG method can generate an accurate solution for the advection equation when the Courant number Cr is unity.

This numerical advantage of the ETG method does not extend for the advection–dispersion equation. Figure 3 illustrates the variations of ζ^h and u^*/u of the ETG method for the advection–dispersion equation over the plane of ωh *vs* Cr corresponding to $Pe = 50$. It is shown from Figure 3 that $\zeta^h \equiv 1$ and $u^*/u \equiv 1$ are no longer satisfied for all the dimensionless wave numbers in $[0, \pi]$ under the condition $Cr = 1$. The fact that amplification factor is greater than unity for certain dimensionless wave numbers will make the numerical scheme unstable in the vicinity of the discontinuity of the solution.

DOI: 10.1002/cnm

5. NUMERICAL ANALYSES

Above observations can be confirmed by numerical evaluations of a one-dimensional linear advective and advective–dispersive transport of a step wave with an advective flow velocity $u = 0.5\,\mathrm{m/s}$. The computational domain is taken as $[0, 30\,\mathrm{m}]$, and it is discretized into 60 elements with an identical elemental length of $h = 0.5\,\mathrm{m}$. Both transport problems have an initial condition of $C = 0$ over the domain, and they are subject to a Dirichlet boundary condition of $C|_{x=0} = 1$ and a Neumann boundary condition of $\partial C/\partial x|_{x=30} = 0$ at the left and right sides of the domain, respectively. First, the ETG method is used to model the advective transport process. Two time steps, $\Delta t = 0.5$ and 1.0 s, are chosen such that the Courant number is equal to $\frac{1}{2}$ and 1 based on the elemental length and the magnitude of the flow velocity. Figure 4 illustrates the computational results for the concentration as the function of the spatial and temporal variables, obtained from the ETG method, corresponding to two different Courant number conditions, i.e. $Cr = \frac{1}{2}$ and 1. From Figure 4, it is evident that the ETG method introduces oscillations into the solution in the vicinity of its the discontinuity for $Cr = \frac{1}{2}$, but it can generate an oscillation-free and non-diffusive solution for advection equation under the condition of $Cr = 1$ because of (23) and (24).

Next, the ETG method is used to simulate an advective–dispersive transport process with a dispersion coefficient $D = 0.005\,\mathrm{m}^2/\mathrm{s}$, giving a Péclet number $Pe = uh/D = 50$ with the same advective flow velocity and using the domain discretization described previously. Again, two time steps, $\Delta t = 0.5$ and 1.0 s, are adopted during the computation to obtain two Courant number conditions, i.e. $Cr = \frac{1}{2}$ and 1. Figure 5 shows the numerical results of this advective–dispersive transport process obtained from the ETG method corresponding to the two Courant number conditions stated above. As expected, severe oscillations are introduced into the solution near its high gradient by the ETG method under the condition of $Cr = 1$ (Figure 5(b)). Such an instability in the computational scheme is due to the fact $\zeta^h > 1$ for certain $\omega h \in [0, \pi]$ with the condition $Cr = 1$. It can be seen from Figure 2(a) that in order to make the ETG scheme stable, the Courant number should be kept less than unity. However, the fact that the amplitude factor is smaller than unity implies that the artificial diffusion will be introduced into the solution by the numerical scheme (see Figure 5(a)). In this case, the numerical oscillations are also introduced by the scheme due to

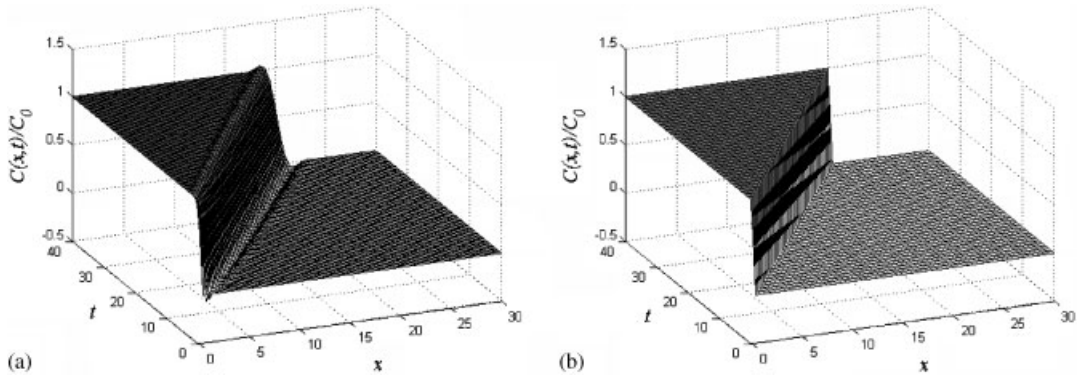

Figure 4. Numerical results for the one-dimensional advective transport problem obtained from the ETG method corresponding to two different Courant numbers: (a) $Cr = 0.5$; and (b) $Cr = 1.0$.

DOI: 10.1002/cnm

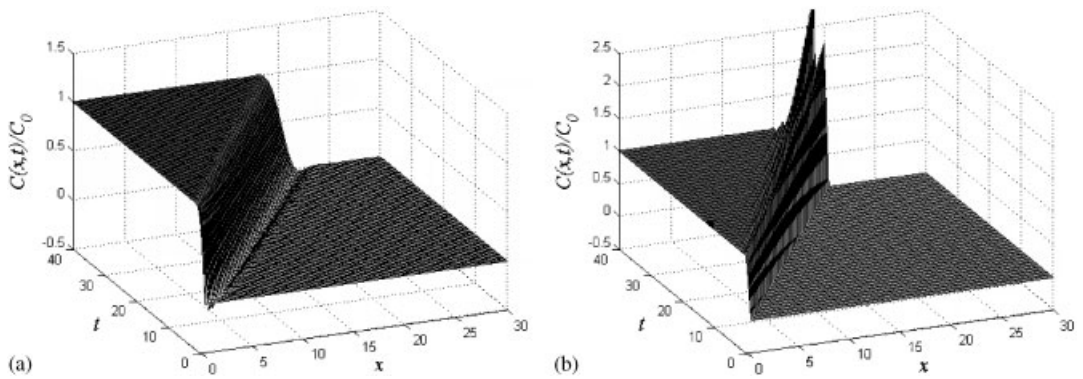

Figure 5. Numerical results for the one-dimensional advective–dispersive transport problem obtained from the ETG method corresponding to two different Courant numbers: (a) $Cr = 0.5$; and (b) $Cr = 1.0$.

the discrepancy between the phase velocity and advective flow velocity for $Cr = \frac{1}{2}$ shown in Figure 2(b).

6. THE OPERATOR-SPLITTING SCHEME FOR THE SPHERICALLY SYMMETRIC TRANSPORT

6.1. The operator-splitting procedure

The fact that the ETG scheme gives accurate solutions for the *advection equation* and unstable solutions for the *advection–dispersion equation* indicates that an operator-splitting procedure needs to be coupled with the ETG scheme to develop an accurate solution for the advection–dispersion equation [23]. Figure 6 illustrates the oscillation-free and non-diffusive numerical solutions, obtained from the operator-splitting ETG scheme, for the one-dimensional advective–dispersive transport process considered in the previous section. In this computation, the advective–dispersive transport is separated into the dispersive part that is solved using the conventional Galerkin method, and advective part that is solved by the ETG method.

Such an operator-splitting numerical scheme can be used to simulate an advection-dominated transport problem from a spherical cavity, which is described by (1)–(3) and (6). In order to utilize the numerical advantage of the ETG method for the advection equation, the spherically symmetric transport problem is computed in the one-dimensional linear space x with the application of the co-ordinate transformation (9), and the transformed transport process is governed by Equation (10). In the operator-splitting modelling, the initial condition of C is transformed into the linear space x with the co-ordinate transformation (9), and the approximation C^{n+1} of the transformed transport process at $t = (n + 1)\Delta t$ is solved in the following two steps: the dispersive process defined by

$$\frac{\partial C_d}{\partial t} - D(3\sqrt[3]{3x})\left(2\frac{\partial C_d}{\partial x} + x\frac{\partial^2 C_d}{\partial x^2}\right) = 0 \qquad C_d|_{t=n\Delta t} = C^n \tag{25}$$

DOI: 10.1002/cnm

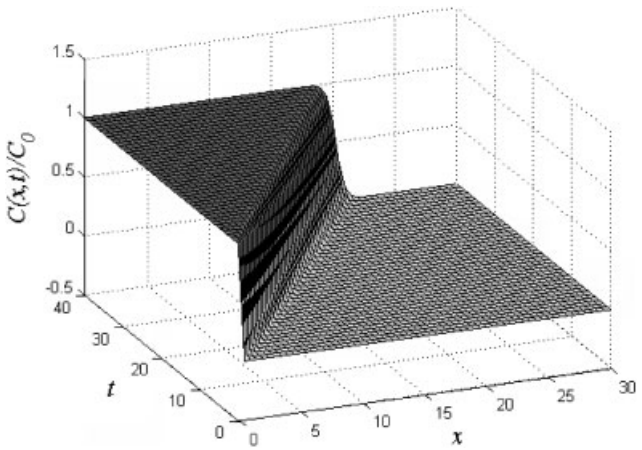

Figure 6. Numerical results obtained from the operator-splitting ETG method for one-dimensional advective–dispersive transport problems with $D = 0.005\ \mathrm{m}^2/\mathrm{s}$.

and the advective process defined by

$$\frac{\partial C}{\partial t} + u\frac{\partial C}{\partial x} = 0 \qquad C|_{t=n\Delta t} = C_d \tag{26}$$

where C^n is the approximation of C at $t = n\Delta t$. It should be noted that since $x > a^3/3$ and $a > 0$, the equation in (25) is parabolic dominant when the spatial discretization is properly chosen. The dispersive process (25) is solved by the conventional Galerkin method, and the advective process (26) is solved by the ETG method. The final results are transformed to the original spherical polar co-ordinate system R with the inverse transformation of (9), i.e. $R = \sqrt[3]{3x}$.

6.2. *Numerical computations*

For the purpose of validation, a spherically symmetric advective transport problem from a spherical cavity will be examined first without considering the contribution from the hydrodynamic dispersion. The contaminant is released from the spherical cavity and transported through a fluid saturated porous region with an established steady radial flow field defined by (6). The spherical cavity has a radius of $a = 3$ m and the Dupuit-Forchheimer hydraulic conductivity of the porous medium is $k = 0.03$ m/day. The boundary of the cavity is subject to a flow potential of $\phi_{\mathrm{p}}(a) = 100$ m and a concentration of $C(a, t) = 1$. The exact closed-form analytical solution for the spherically symmetric advective transport in a porous medium of infinite extent was given by Selvadurai [24] and takes the form

$$\frac{C(R, t)}{C_0} = \mathsf{H}[1 - \lambda(\rho)] \tag{27}$$

DOI: 10.1002/cnm

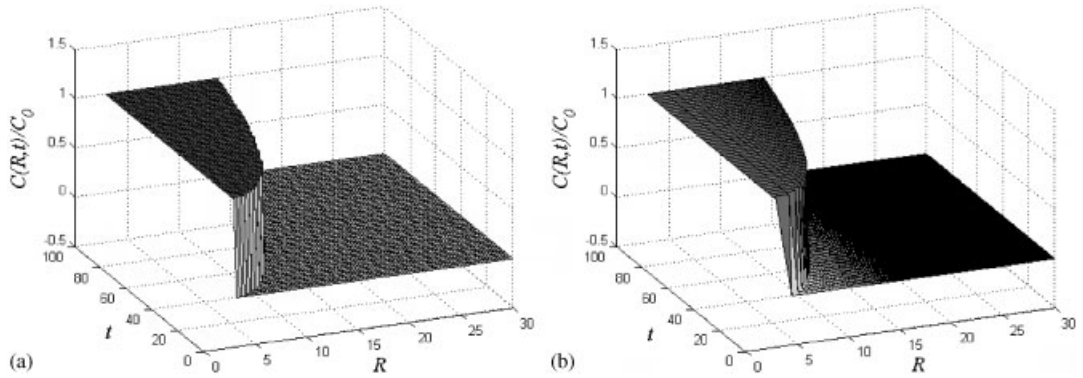

Figure 7. The analytical and numerical solutions of the spherically symmetric advective transport problem with a stationary flow field during a 100 day period: (a) analytical solution; and (b) numerical solution.

where

$$\lambda(\rho) = \frac{a^2}{3\phi_0 k}[\rho^3 - 1]; \quad \rho = \frac{R}{a}$$

Figure 7(a) shows the results obtained from the analytical solution (27) over a 100-day period.

In the numerical computations, the porous medium of infinite extent is represented by a finite region $a \leqslant R \leqslant b$ and $b = 30$ m. A homogeneous Neumann boundary condition is applied on outer boundary, i.e. $\partial C/\partial R|_{R=b} = 0$, to replace the regularity condition at the infinite location. The ETG method along with the use of the co-ordinate transformation (9) is used to model this spherically symmetric advective transport problem. It should be noted that the radial flow velocity (6) has a strong spatial dependency, but such dependency is eliminated in the linear space x through the use of the co-ordinate transformation (9). Since the transformed flow velocity u is a constant, the time step is chosen based on the Courant number criterion $Cr = 1$ during the computations in the one-dimensional linear space x. The corresponding computational results for the spherically symmetric advective transport problem are shown in Figure 7(b). From Figure 7, it is evident that the piecewise element in linear space x is refined at far field in the original spherical polar co-ordinate R, where the magnitude of the flow velocity is smaller. Figure 8 indicates the comparison of migration of the discontinuous edge of the contaminant concentration with time along the radial direction, as obtained from the ETG scheme and that obtained from the analytical solution (27). In Figure 8, R_1 and R_2 represent the near and far ends of the element where the discontinuity of the solution is located, and therefore they approach each other when the element size decreases.

Next, the above contaminant transport process with the consideration of both advective and dispersive contributions from the spherical cavity in the spherically symmetric homogeneous porous region is computed by the operator-splitting ETG modelling described in the previous section. The dispersion coefficient is assumed to be $D = 0.05\ \mathrm{m}^2/\mathrm{s}$, and the other parameters and boundary conditions related to the transport process are kept the same as ones defined previously. The time step is chosen based on the Courant number criterion $Cr = 1$ in the linear space x. The corresponding oscillation-free computational results are shown in Figure 9, which indicate the

DOI: 10.1002/cnm

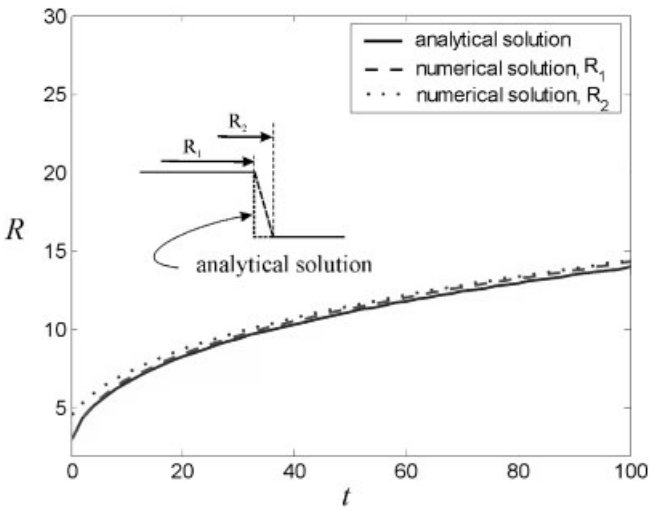

Figure 8. Comparison of the migrations of step concentration profile along the radial direction obtained from the numerical and analytical solutions.

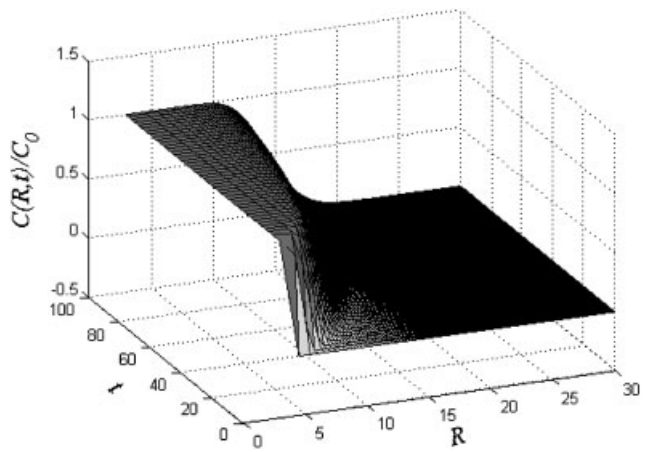

Figure 9. Numerical results for the spherically symmetric advective–dispersive transport with a constant dispersion coefficient $D = 0.05\ \mathrm{m}^2/s$, obtained from the operator-splitting ETG method ($Cr = 1$).

accuracy and efficiency of the proposed operator-splitting ETG scheme for solving the spherically symmetric advection-dominated transport problem.

7. CONCLUSIONS

An operator-splitting Euler–Taylor–Galerkin (ETG) method is used to develop an oscillation-free and non-diffusive computational solution for the advective–dispersive migration of a contaminant

DOI: 10.1002/cnm

from a spherical source in a homogeneous fluid-saturated porous region. A Fourier analysis of the ETG method for the classical advection–dispersion equation is used as the justification for the development of an operator-splitting approach. It is shown from the Fourier analysis that the ETG scheme can give an oscillation-free and non-diffusive solution for the advection equation when the Courant number $Cr = 1$, but such numerical advantage does not extend to the advection–dispersion equation. This conclusion is verified by the numerical computations of advection and advection–dispersion problems involving a migrating front with a discontinuous leading edge. Based on this observation, an operator-splitting ETG scheme has been developed for modelling the spherically symmetric advective–dispersive transport problem in a porous medium containing a cavity. In the numerical modelling, a co-ordinate transformation is applied to spherically symmetric transport equation to generate a one-dimensional advection–dispersion equation with a constant advective velocity for the purpose of using the numerical advantage of the ETG method for the one-dimensional advection equation. Computational results derived from the operator-splitting ETG method compare closely with a known exact closed-form analytical solution.

REFERENCES

1. Bear J, Verruijt A. *Modeling Groundwater Flow and Pollution*. D. Reidel Publishing Co.: Dordrecht, The Netherlands, 1990.
2. Bedient PB. *Ground Water Contamination*: *Transport and Remediation*. Prentice-Hall: Upper Saddle River, NJ, 1999.
3. Bear J, Bachmat Y. *Introduction to the Modeling of Transport Phenomena in Porous Media*. D. Reidel Publishing Co.: Dordrecht, The Netherlands, 1992.
4. Lewis RW, Schrefler BA. *The Finite Element Method in the Static and Dynamic Deformation and Consolidation of Porous Media*. Wiley: New York, 1998.
5. Vichnevetsky R, Bowles JB. *Fourier Analysis of Numerical Approximations of Hyperbolic Equations*. SIAM: Philadelphia, PA, 1982.
6. Raymond WH, Garder A. Selective damping in a Galerkin method for solving wave problems with variable grids. *Monthly Weather Review* 1976; **104**:1583–1590.
7. Pereira JMC, Pereira JCF. Fourier analysis of several finite difference schemes for the one-dimensional unsteady convection–diffusion equation. *International Journal for Numerical Methods in Fluids* 2001; **36**:417–439.
8. Hauke G, Doweidar MH. Fourier analysis of semi-discrete and space-time stabilized methods for the advective–diffusive–reactive equation: II SGS. *Computer Methods in Applied Mechanics and Engineering* 2005; **194**:691–725.
9. Selvadurai APS, Dong W. A time adaptive scheme for the accurate solution of the advection equation with a transient flow velocity. *Computer Modeling in Engineering and Sciences* 2006; **12**:41–54.
10. Dong W. Modeling of advection-dominated transport in fluid-saturated porous media. *Ph.D. Thesis*, McGill University, 2006.
11. Hughes TJR. Multiscale phenomena: Green functions, the Dirichlet-to-Neumann formulation, subgrid scale models, bubbles, and the origins of stabilized methods. *Computer Methods in Applied Mechanics and Engineering* 1995; **127**:387–401.
12. Brezzi F, Bristeau MO, Franca LP, Mallet M, Rogé G. A relationship between stabilized finite element methods and the Galerkin method with bubbles for advection–diffusion problems. *Computer Methods in Applied Mechanics and Engineering* 1992; **96**:117–129.
13. Brezzi F, Franca LP, Hughes TJR, Russo A. '$b = \int g$'. *Computer Methods in Applied Mechanics and Engineering* 1997; **145**:329–339.
14. Franca LP, Farhat C. Bubbles functions prompt unusual stabilized finite element methods. *Computer Methods in Applied Mechanics and Engineering* 1995; **123**:299–308.
15. Franca LP, Hwang F. Refining the submesh strategy in the two-level finite element method: application to the advection–diffusion equation. *International Journal for Numerical Methods in Fluids* 2002; **39**:161–187.
16. Codina R. Comparison of some finite element methods for solving the diffusion–convection–reaction equation. *Computer Methods in Applied Mechanics and Engineering* 1998; **156**:185–210.

DOI: 10.1002/cnm

17. Hughes TJR, Brooks A. A theoretical framework for Petrov–Galerkin methods with discontinuous weighting functions: application to the streamline-upwind procedure. In *Finite Elements in Fluids*, Gallagher RH *et al.* (eds), vol. 4. Wiley: Chichester, 1982; 47–65.
18. Carey GF, Jiang BN. Least square finite element method and pre-conditioned conjugate gradient solution. *International Journal for Numerical Methods in Engineering* 1987; **24**:1283–1296.
19. Donea J, Giulian S, Laval H, Quartapelle L. Time-accurate solution of advection–diffusion problem by finite elements. *Computer Methods in Applied Mechanics and Engineering* 1984; **45**:123–145.
20. Donea J, Quartapelle L, Selmin V. An analysis of time discretization in the finite element solution of hyperbolic problems. *Journal of Computational Physics* 1987; **70**:463–499.
21. Oñate E, García J, Idelsohn S. Computation of the stabilization parameter for the finite element solution of advective–diffusive problems. *International Journal for Numerical Methods in Fluids* 1997; **25**:1385–1407.
22. Lax PD, Wendroff B. Systems of conservation laws. *Communications on Pure and Applied Mathematics* 1960; **13**:217–237.
23. Wendland E, Schmid GA. Symmetrical streamline stabilization scheme for high advective transport. *International Journal for Numerical and Analytical Methods in Geomechanics* 2000; **24**:29–45.
24. Selvadurai APS. The advective transport of a chemical from a cavity in a porous medium. *Computers and Geotechnics* 2002; **29**:525–546.

DOI: 10.1002/cnm